International Journal of Research Studies in Agricultural Sciences (IJRSAS)
Volume 4, Issue 6, 2018, PP 8-22
ISSN No. (Online) 2454–6224
DOI: http://dx.doi.org/10.20431/2454-6224.0406002
www.arcjournals.org

Comparison of C3 and C4 Plants Metabolic

Hamid kheyrodin

Assistant professor in Semnan University, Iran

Corresponding Author:** ***Hamid kheyrodin, *Assistant professor in Semnan University, Iran*

Abstract: *C4 carbon fixation or the Hatch–Slack pathway is a photosynthetic process in some plants. It is the first step in extracting carbon from carbon dioxide to be able to use it in sugar and other biomolecules. It is one of three known processes for carbon fixation. The C4 in one of the names refers to the four-carbon molecule that is the first product of this type of carbon fixation. C4 fixation is an elaboration of the more common C3 carbon fixation and is believed to have evolved more recently. C4 overcomes the tendency of the enzyme RuBisCO to wastefully fix oxygen rather than carbon dioxide in the process of photorespiration.*

The C4 photosynthetic cycle supercharges photosynthesis by concentrating CO2 around ribulose-1,5-bisphosphate carboxylase and significantly reduces the oxygenation reaction. Therefore engineering C4 feature into C3 plants has been suggested as a feasible way to increase photosynthesis and yield of C3 plants, such as rice, wheat, and potato. To identify the possible transition from C3 to C4 plants, the systematic comparison of C3 and C4 metabolism is necessary.

1. Introduction and Background

The first experiments indicating that some plants do not use C_3 carbon fixation but instead produce malate and aspartate in the first step of carbon fixation were done in the 1950s and early 1960s by Hugo P. Kortschakand Yuri Karpilov. The C_4 pathway was elucidated by Marshall Davidson Hatch and C. R. Slack, in Australia, in 1966; it is sometimes called the Hatch-Slack pathway.

C4 plants such as maize, sorghum, and sugarcane, approximately have 50% higher photosynthesis efficiency than those of C3 plants such as rice, wheat, and potato [1]. This is because the different mechanism of carbon fixation by the two types of photosynthesis, as illustrated in Figure Figure1.1. C3 photosynthesis only uses the Calvin cycle for fixing CO_2 catalyzed by ribulose-1,5-bisphosphate carboxylase (Rubisco), which takes place inside of the chloroplast in mesophyll cell. For C4 plants such as maize (NADP-ME subtype), photosynthetic activities are partitioned between mesophyll and bundle sheath cells that are anatomically and biochemically distinct. The initial carbon fixation is catalyzed by phosphoenolpyruvate carboxylase (PEPC) forming oxaloacetate (OAA) from CO_2 and phosphoenolpyruvate (PEP). OAA is metabolized into malate, and then diffuses into the BS cell where it is decarboxylated to provide increased concentration of CO_2 around Rubisco. Finally, the initial substrate of the C4 cycle, PEP, is regenerated in mesophyll cell by pyruvate orthophosphate dikinase (PPDK) [1]. The CO_2 concentration mechanism suppresses the oxygenation reaction by Rubisco and the subsequent energy-wasteful photorespiratory pathway, resulting in increased photosynthetic yield and more efficient use of water and nitrogen comparing to C3 plants [2]. Therefore genetic engineering of C4 features into C3 plants such as rice (Oryza sativa) has the potential to increase crop productivity [3-5]. However, attempts to use these tools to engineer plant metabolism have met with limited success due to the complexity of plant metabolism. Genetic manipulations rarely cause the predicted effects, and new rate-limiting steps prevent the accumulation of some desired compounds [6,7].

In a bid to improve our understanding of plant metabolism and thereby the success rate of plant metabolic engineering, a systems-based framework to study plant metabolism is needed [7,8]. Systems biology involves an iterative process of experimentation, data integration, modeling, and generation of hypotheses [9,10]. With the recent advancement of genome sequencing, several plants have complete genomic sequence and annotation, including Arabidopsis (Arabidopsis thaliana) [11],

rice (Oryza sativa), sorghum (Sorghum bicolor) [12], and maize (Zea mays), which make it possible to reconstruct the genome-scale metabolic network of plants.

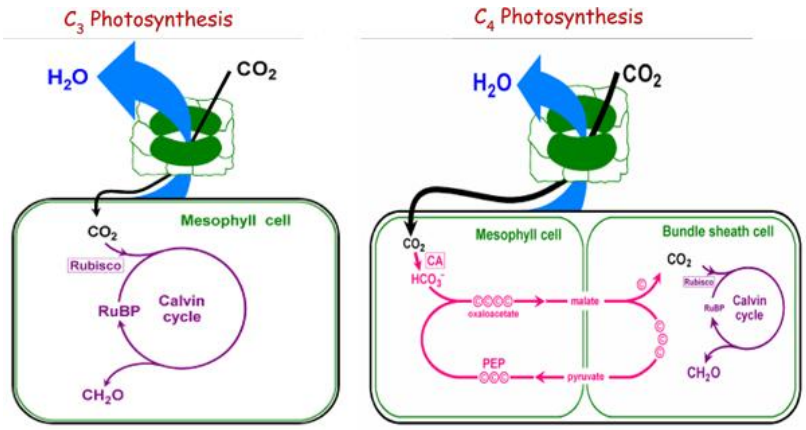

Figure1. *A Schematic Diagram of C3 and C4 Photosynthesis*

Constraint-based model, also called Flux Balance Analysis (FBA), is a useful method to analyze large-scale metabolic network without requiring detail kinetic parameters. In FBA, flux states are predicted which are optimal with regard to an assumed cellular objective such as maximizing biomass yield [13-16]. For microbial organisms, FBA has been successful in predicting *in vivo* maximal growth rate, substrate preference and the requirement for particular biochemical reactions for cellular growth [17]. For plants, highly compartmentalized stoichiometric models have been developed for barley seeds [18] and Chlamydomonas [14], especially several models have been reported for Arabidopsis [19-22]. In addition, the analysis of metabolic network for photosynthetic bacteria has also been conducted, such as Synechocystis [23] and purple nonsulfur bacteria [24].

The genome scale metabolism models of C3 plant Arabidopsis [19] and C4 plant [25] have been constructed, but no comparative analysis between them. In this study, we improved the two models, AraGEM and C4GEM, by setting ratio of carboxylation and oxygenation by Rubisco, and compared the differences of network structure and metabolic flux to elucidate the evolutionary significance. We explored the effects of enzyme knockouts on photosynthesis and biomass synthesis, and compared the contribution of different C4 subtypes to biomass production. In addition, we revealed the different response to environment conditions in C3 and C4 plants. The system flow of our analysis is shown in Figure Figure2.2. This study will shed light on the metabolism changes from C3 to C4 at systems level, which is important for feasible engineering of C3 to C4 plants.

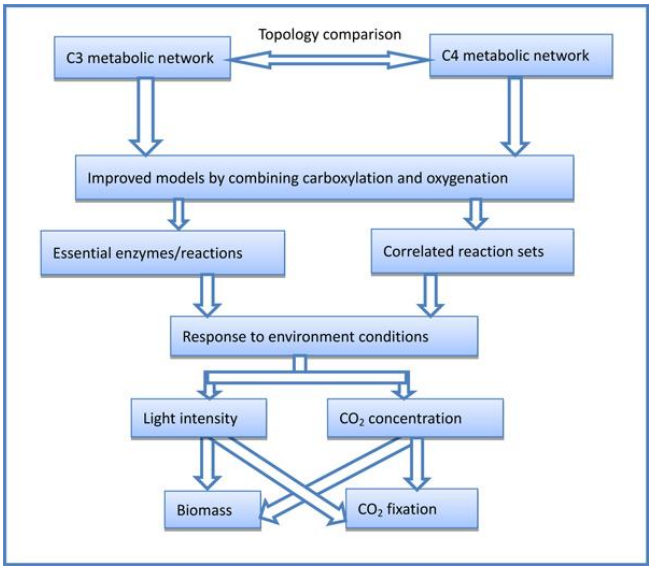

Figure2. *System flow of the comparison between C3 and C4 metabolic networks*

2. Results and Discussion

2.1. Topological Characteristics of C3 and C4 Metabolic Networks

The metabolism model of Arabidopsis AraGEM includes 1498 unique reactions, 1765 metabolites, 83 inter-organelle transporters, and 18 inter-cellular transporters [19]. For the metabolism model of C4 plants C4GEM, there are 2377 reactions, 2886 metabolites, 177 inter-organelle transporters, and 23 external transporters [25]. The topological properties of AraGEM and C4GEM models were analyzed using pajek [26], where reactions are represented as nodes and metabolites as edges. Some important topological parameters such as average degree, betweenness centrality, average clustering coefficient and distance were compared between these two models, as shown in Table Table1.The1.The results demonstrated that the Ara GEM has a more dense structure than C4GEM, because C3 plant is single-cell, while C4 plant consists of mesophyll cell and bundle sheath cell, the connections between two-cells are not as close as single-cell. Then we extracted the primary metabolism from C3 and C4 networks, including Calvin cycle, photorespiration, TCA cycle, nitrogen metabolism, sucrose and starch metabolism, and some major amino acid metabolism pathways. Using NET-SYNTHESIS [27], we calculated the redundancy of primary metabolic network of C3 and C4, which is 0.7175 and 0.7606 respectively. It means C4 network is more redundant so that C4 plant could be more robust to gene mutation or environment changes.

Table1. *Topological properties of AraGEM and C4GEM*

model	Average Degree	Degree Centralization	Average Clustering Coefficient	Betweenness Centralization	Average distance	Maximum distance	Redundancy of primary network
C3	91	0.24016	0.37978	0.04336	2.75825	11	0.7175
C4	56	0.11384	0.40274	0.15158	3.58215	14	0.7606

2.2. Improved Models by Setting the Ratio of Carboxylation and Oxygenation by Rubisco

Rubisco enzyme (EC: 4.1.1.39) catalyzed two different reactions with CO_2 and O_2 respectively in photosynthesis and photorespiration:

$$RuBP + CO_2 + H_2O \text{ - > } 2PGA \quad (1)$$

$$RuBP + O_2 \text{ - > } PGA + PGCA \quad (2)$$

There is constant ratio between rate of carboxylation and oxygenation under specific partial pressure of CO_2 and O_2 in environment [28]. Therefore, it is hard to accurately simulate the flux change under different CO_2 concentration without constraints on rate of the two reactions by Rubisco, which is just the limitation of AraGEM and C4GEM. Here we improved the two models by combining the two reactions into one reaction:

$$(r + 1)RuBP + r\,CO_2 + r\,H_2O + O_2 \text{ - > } (2r + 1)\,PGA + PGCA \quad (3)$$

The ratio r between carboxylation and oxygenation under different CO_2 concentration in C3 and C4 model is shown in Table Table2.2. The detail calculation of r is in the Methods section.

Table2. *The ratio r between carboxylation and oxygenation under different CO_2 concentration in C3 and C4 model*

CO_2 (μbar) in the air	*r* in C3	*r* in C4
100	1.139	22.2282
380	4.33	70.7281
550	6.26	85.9654
800	9.11	87.1062
1000	11.39	88.0189

In addition, our motivation was to compare the differences between C3 and C4 photosynthesis mechanism and their responses under different environments, therefore we set the objective function as maximization of CO_2 fixation and biomass synthesis. Since in previous AraGEM and C4GEM, the objective was to minimize the use of light energy while achieving a specified growth rate, we need to reset some flux constraints according to biochemistry knowledge. For example, the CO_2 leakage was blocked from bundle sheath to mesophyll cell with zero flux in C4GEM, which was not consistent with actual situation; here we adjusted the upper bound of this reaction to permit the leakage of CO_2.

In addition, because starch is not synthesized in mesophyll cell of C4 plants, the biomass components of C4GEM were also reset. The lower and upper bounds of flux in TCA cycle were adjusted as -50 and 50, to restrict flux of respiration in mitochondria. The detail of modified constraints in our improved models can be got from the Additional File.

2.3. The Effects of Knock-Out Enzymes on Metabolic Flux

Based on the improved C3 and C4 metabolic networks, we compared the optimal flux of biomass synthesis and CO_2 fixation using FBA. When biomass synthesis is the objective function, the maximal flux of biomass is 3.661 and 4.625 $mmol \cdot gDW^{-1} \cdot hr^{-1}$ respectively in C3 and C4 networks. Similarly, when optimizing CO_2 fixation, the maximal flux is 200.95 $mmol \cdot gDW^{-1} \cdot hr^{-1}$ in C3 network and 387.619 $mmol \cdot gDW^{-1} \cdot hr^{-1}$ in C4 network. It demonstrated that C4 network exhibited both higher fluxes of biomass and CO_2 fixation than C3 network, which was consistent with the actual tendency. We concluded that the two genome-scale metabolic networks could explain actual situations and be compared for understanding the similarities and differences of C3 and C4 plants.

Next, we evaluated the effects of enzyme knockouts on flux of CO_2 fixation and biomass. When one enzyme was knockout, its corresponding reactions would be deleted, which resulted in changes of the optimal flux of biomass or CO_2 fixation. The objective results from the simulation were classified as unchanged objective (ratio = 1), reduced objective (ratio $\in$ (0, 1)) and no objective (ratio = 0). The effects of single reaction deletion on maximal flux of biomass in C3 and C4 network are shown in Table Table3.3. More than 85% reactions have no effects on the maximal biomass of C3 and C4 network when being knocked-out, so we concluded that the two networks have amazing robustness. Almost 10% of the reactions would result in zero biomass in C3 and C4 networks, which include some important transporters. The single deletion of important reactions or enzymes such as phosphoribulokinase (PRK, EC: 2.7.1.19) and light reactions can result in no biomass, which is consistent with the real characteristics of plants [29].

Table3. *The effects of knockout reactions on maximal flux of biomass*

Ratio of objective flux	C3 reactions		C4 reactions	
	Number	Percentage	Number	Percentage
Ratio ≈0	169	10.58%	236	9.16%
0<Ratio<0.90	14	0.88%	6	0.23%
0.90<Ratio<1	37	2.32%	78	3.03%
Ratio = 1	1378	86.23%	2256	87.58%

The effects of single reaction deletion on C3 and C4 networks when objective function is CO2 fixation are shown in Table Table44 which is similar with Table Table3.3. More than 96% reactions have no influence on the maximal flux of CO_2 fixation when being deleted in C3 and C4 networks. We concluded that more reactions have no influence on the maximal flux of CO_2 fixation than biomass. Since biomass synthesis includes many components which deal with more than one reaction, their deletion will affect the flux of biomass synthesis. In addition, it is obvious that C4 plants exhibit much better robustness than C3 plants, since higher percentage of enzyme knockouts result no change on the objective flux and lower percentage result in zero flux. Moreover, we found all the essential reactions in C3 network are also essential for C4, while there are some other reactions specifically essential for C4. This result proved that the basic metabolism of C4 plants was similar to C3, but C4 became more complex during long period of evolution.

Table4. *The effects of knockout reactions on maximal flux of CO_2 fixation*

Ratio of objective flux	C3 reactions		TC4 reactions	
	Number	Percentage	Number	Percentage
Ratio ≈0	16	1.00%	19	0.74%
0<Ratio<0.90	26	1.63%	25	0.97%
0.90<Ratio<1	18	1.13%	16	0.62%
Ratio = 1	1538	96.25%	2516	97.67%

We found there are some gaps in C4GEM when checking the xylose pathway in the two networks. In AraGEM, there are two pathways to produce xylose, so knockout of UDP-glucose 6-dehydrogenase (UDPGDH, EC:1.1.1.22) will not influence on the biomass synthesis. But in C4GEM, only UDPGDH was responsible for xylose production, the other alternative pathway does not work because of two

missing enzymes, xylose isomerase (EC: 5.3.1.5) and xylulokinase (EC:2.7.1.17). We searched the GeneBank database [30] to find that genes (GeneID: 100194128, 100194385) encoding xylose isomerase and genes (GeneID: 100282641, 100382670) encoding xylulokinase. So we complemented the xylose pathway in C4GEM, thus the biased results can be avoided.

Next we investigated the effects of particular key enzymes on photosynthesis and biomass synthesis in C3 and C4 plants. Table Table55 illustrated these enzymes, their functions and the ratio of objective flux after deletion. '0' means the knocked-out enzyme resulting no flux of biomass or CO_2 fixation, while '1' means there is no influence on maximal flux of biomass or CO_2 fixation. Knockouts of enzymes in Calvin cycle have lethal effects on both C3 and C4 networks. For example, the central enzyme of Calvin cycle, Rubisco (EC: 4.1.1.39) catalyzes the fixation of both CO_2 and O_2. Its deletion results in zero flux of CO_2 fixation and biomass, which accords with the fact that photosynthesis and plant growth is positively correlated with Rubisco activity [31,32]. When deleting transaldolase (TAL, EC: 2.2.1.2) in pentose phosphate pathway and glycolate oxidase (LOX, EC: 1.1.3.15) in glyoxylate and dicarboxylate metabolism pathway, the CO2 fixation and biomass will also reduce to zero flux in these two plants [33,34]. Aconitases (EC: 4.2.1.3) is an important enzyme in TCA cycle, its knockout reduced the flux of CO_2 fixation, and completely no flux of biomass in both C3 and C4 networks [35].

Table5. *The effects of key enzyme knockouts on optimal flux of biomass and CO2 fixation*

Enzyme	**EC**	**Pathway**	**Ratio of biomass**		**Ratio of CO_2 fixation**	
			C3	**C4**	**C3**	**C4**
Rubisco	4.1.1.39	Calvin cycle	0	0	0	0
RPI	5.3.1.6	Calvin cycle	0	0	0	0
Prk	2.7.1.19	Calvin cycle	0	0	0	0
RPE	5.1.3.1	Calvin cycle	0	0	0	0
TKT	2.2.1.1	Calvin cycle	0	0	0	0
TAL	2.2.1.2	Pentose phosphate pathway	0	0	0	0
LOX	1.1.3.15	Glyoxylate and dicarboxylate metabolism	0	0	0	0
Aconitases	4.2.1.3	TCA cycle	0	0	0.89	0.82
PGLP	3.1.3.18	Photorespiratory	1	1	1	1
SPP	3.1.3.24	Sucrose biosynthesis	1	1	1	1
Amylase isomerase	2.4.1.18	Transitory starch biosynthesis	0	0	1	1
PEPC	4.1.1.31	C4 photosynthesis	1	0	1	1
PPDK	2.7.9.1	C4 photosynthesis	1	0.96	1	0.98

The knockout of hosphoglycolate phosphatase (PGLP, EC: 3.1.3.18) has no effect on the CO_2 fixation and biomass synthesis, because it catalyzes the first reaction of the photo respiratory C2 cycle [36]. Sucrose-6(F)-phosphate phosphohydrolase (SPP, EC: 3.1.3.24) catalyzes the final step in the pathway of sucrose biosynthesis [37]. Its deletion has no influence, because sucrose synthesis locates in cytosol and has no direct connection with photosynthesis. Amylase isomerase (EC: 2.4.1.18) is responsible for the synthesis of transitory starch in chloroplast, which is the critical reaction for the normal biosynthesis of storage starch, so its deletion has lethal effect on biomass flux for both C3 and C4 plants [38].

In C4 plants, Phosphoenolpyruvate carboxylase (PEPC, EC: 4.1.1.31) notably performs the initial fixation of atmospheric CO_2 in photosynthesis, which catalyzes the carboxylation of phosphoenolpyruvate (PEP) in a reaction that yields oxaloacetate and inorganic phosphate [39]. Therefore, knockout of PEPC resulted in zero flux of biomass, which validates its crucial role in C4 photosynthesis. Pyruvate phosphate dikinase (PPDK, EC: 2.7.9.1) catalyzes the conversion of the 3-carbon compound pyruvate into phosphoenolpyruvate. Its deletion reduced the flux of CO_2 fixation and biomass, which is consistent with experiment results that inhibition of PPDK significantly hinders C4 plant growth [40]. In comparison, these two enzymes have no effect on CO_2 fixation and biomass in C3 network.

2.4. Correlated Reaction Sets Identified by Sampling

There are some reactions co-utilized in precise stoichiometric ratios and exhibit correlated flux in the metabolic network, which called correlated reaction sets. We used the uniform random sampling method to determine dependencies between reactions which can be further used to define modules of reactions [See Methods section]. The simplified model of the C3 network has 494 reactions, 483 metabolites and narrow range on constraints, which can be separated into 65 modules and the largest module consists of 92 reactions. The simplified model of the C4 network has 826 reactions, 806 metabolites and narrow range on constraints, which can be separated into 113 modules and the largest module consists of 169 reactions. There are more correlated reaction sets in C4 than C3 network.

The fluxes of reactions in the same module exhibit linear correlation. We found the reactions in Calvin cycle are correlated in both C3 and C4 network, as illustrated in Figure Figure33 and and44 respectively. However, there are some reactions from different pathways also exhibit linear correlation in C4 network, but they are not correlated in C3 model. For example, the reactions from Sugar metabolism, Stibene, counarine and lignin biosynthesis, and Coumarine and phenylpropanoid biosynthesis pathways are significantly correlated in C4 (shown in Figure Figure5),5), but no correlation among them in C3 (shown in Figure Figure6).6). It demonstrated that C4 plants have better modularity with complex mechanism coordinates the reactions and pathways than that of C3 plants.

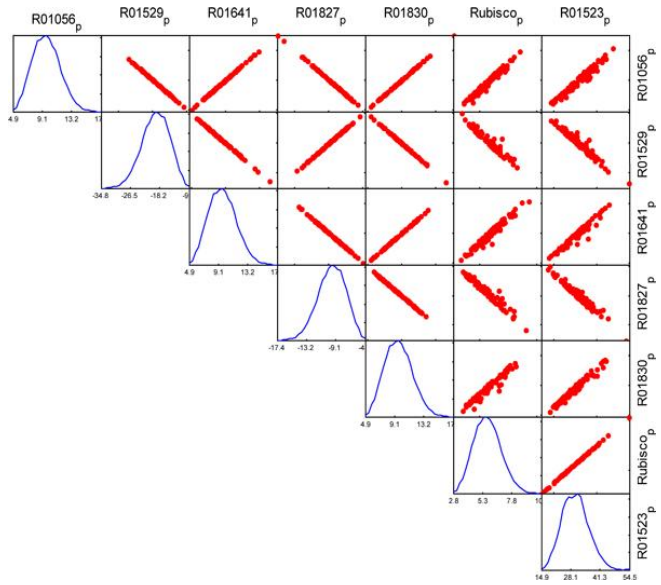

Figure3. *Correlated reaction sets of Calvin cycle in C3 network.*

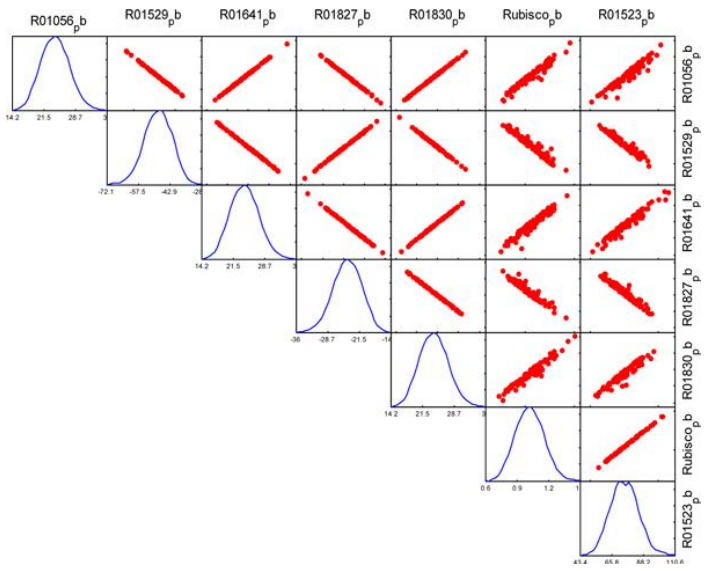

Figure4. *Correlated reaction sets of Calvin cycle in C4 network*

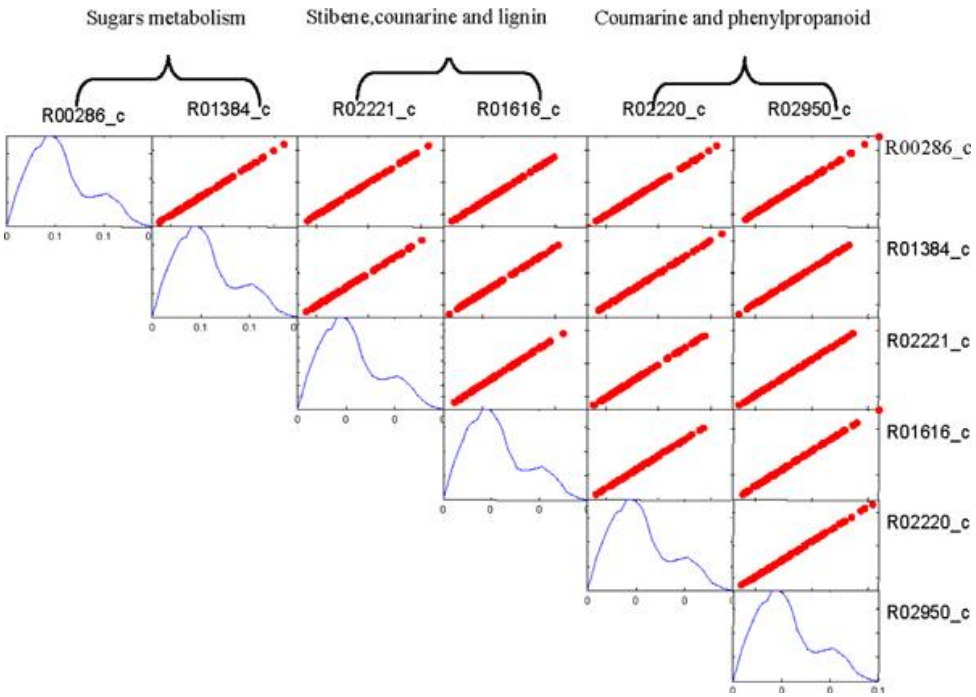

Figure5. *The reactions from several pathways are correlated in C4 network*.

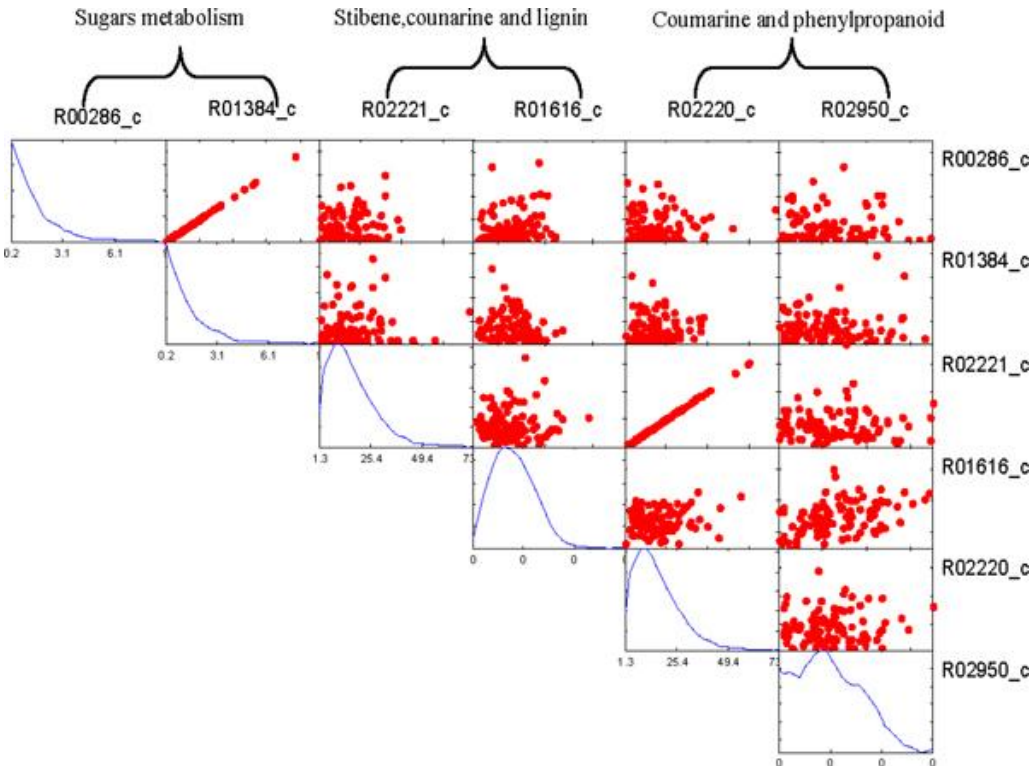

Figure6. *The reactions from several pathways same with C4 are not correlated in C3 network*.

2.5. Comparison of Response to Different Environment Conditions

The biomass and CO_2 fixation of C3 and C4 models were simulated under different light intensity, as shown in Figure Figure77 and and8.8. The C3 model (red in Figure Figure7)7) and C4 model (blue in Figure Figure7)7) presented linear relationship between biomass and light intensity when light intensity is less than 1500. Then with the light intensity increasing, the biomass would be unchanged in C4 model and still increased in C3 model. The C3 model (red in Figure Figure8)8) and C4 model (blue in Figure Figure8)8) also presented linear relationship between CO_2 fixation and light intensity when light intensity is less than 1600. Then the CO_2 fixation was almost keeping unchanged. The

increase of both biomass and CO_2 fixation with light intensity in C4 are faster than that in C3, which reflect more efficient use of solar energy in C4 plants [41]. In addition, we simulated the flux of biomass synthesis and CO_2 fixation under different CO_2 concentration, as shown in Figure Figure99 and and10.10. The more CO2 concentration increases, the more flux of biomass and CO_2 fixation, and the increase gradually change slowly until to steady state. The simulated curve was consistent with experiment *A-Ci* curve [42]. We found that the increase of both biomass and CO_2 fixation with CO_2 concentration in C4 are faster than that in C3, which reflect more efficient use of CO_2 in C4 plants.

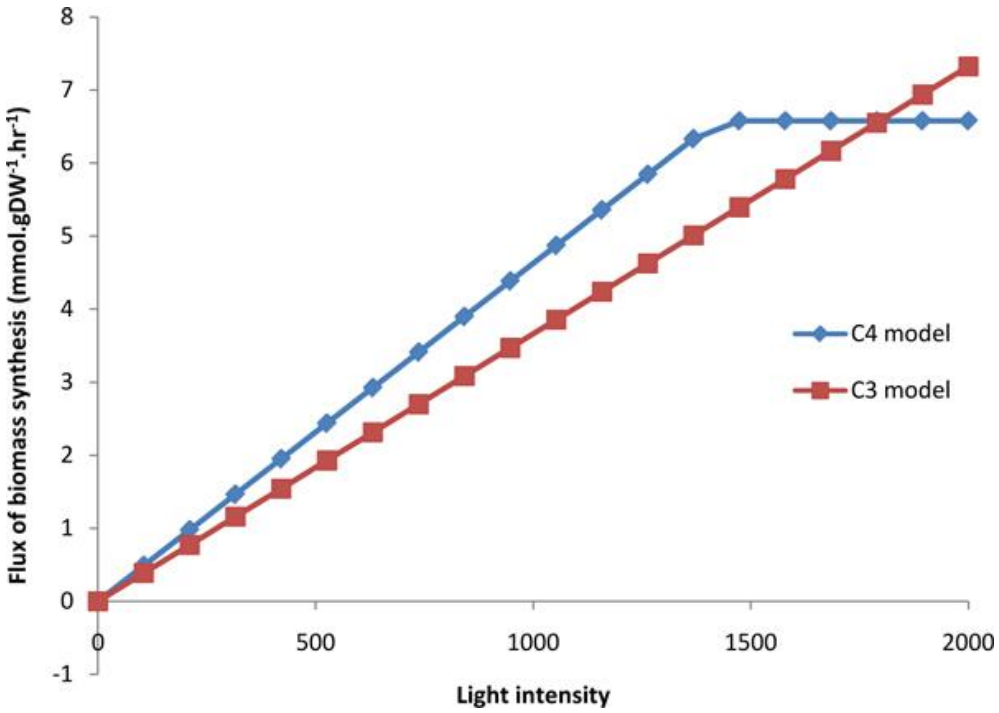

Figure7. *The effect of light intensity on biomass synthesis in C3 and C4 model*

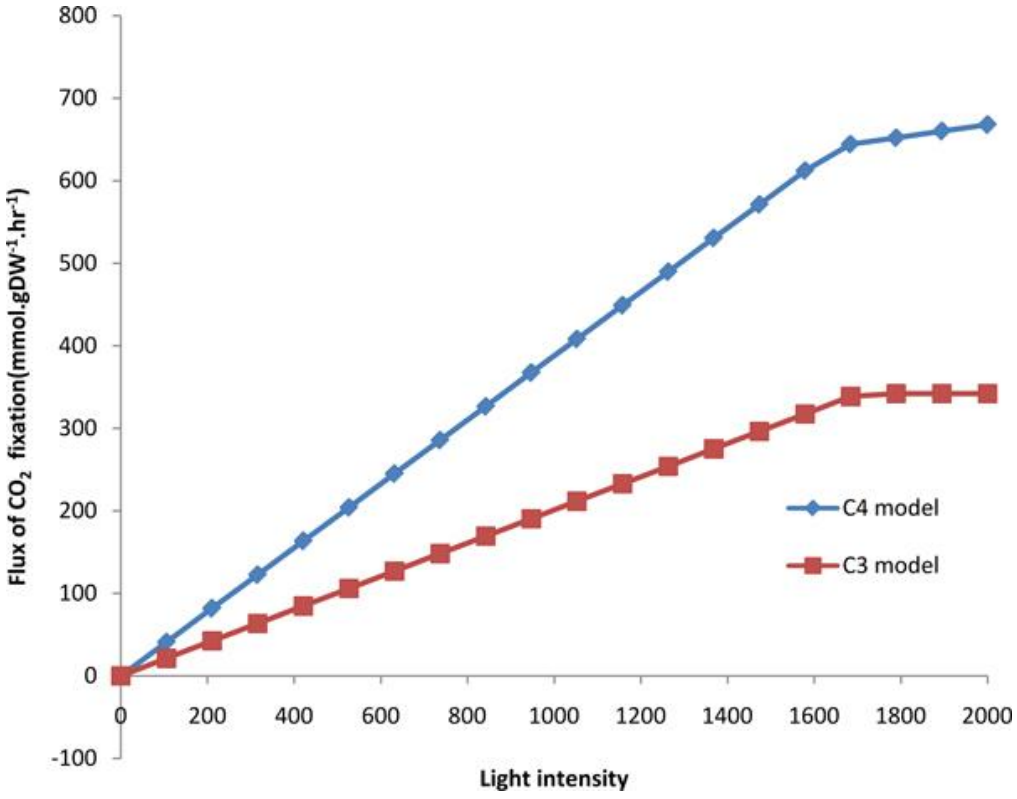

Figure8. *The effect of light intensity on CO_2 fixation in C3 and C4 model*

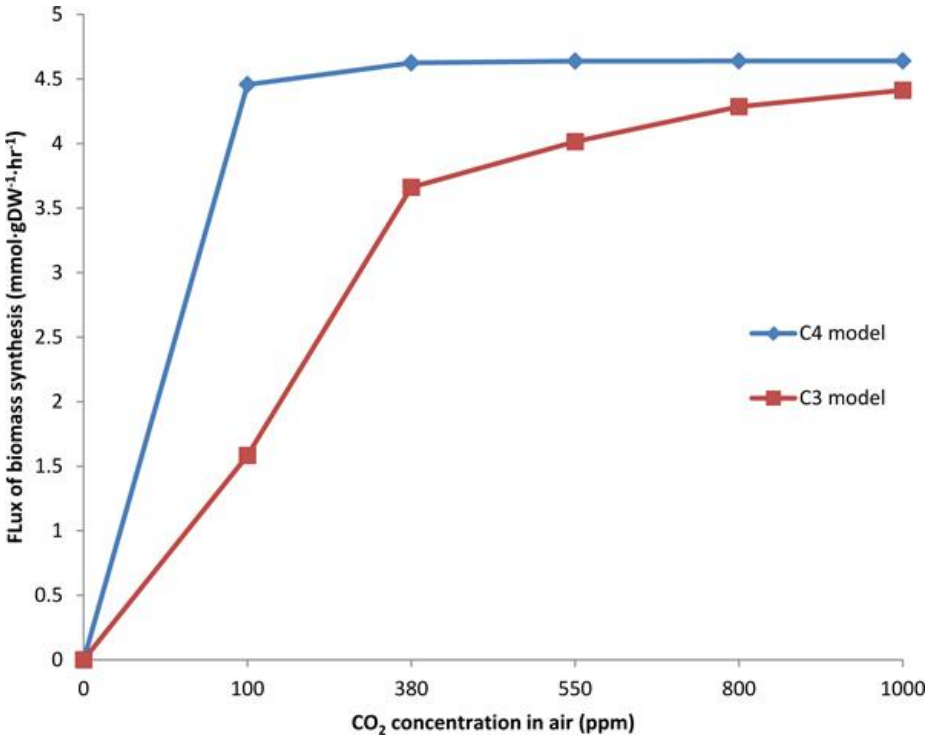

Figure9. *The effect of CO_2 concentration on biomass synthesis in C3 and C4 model*

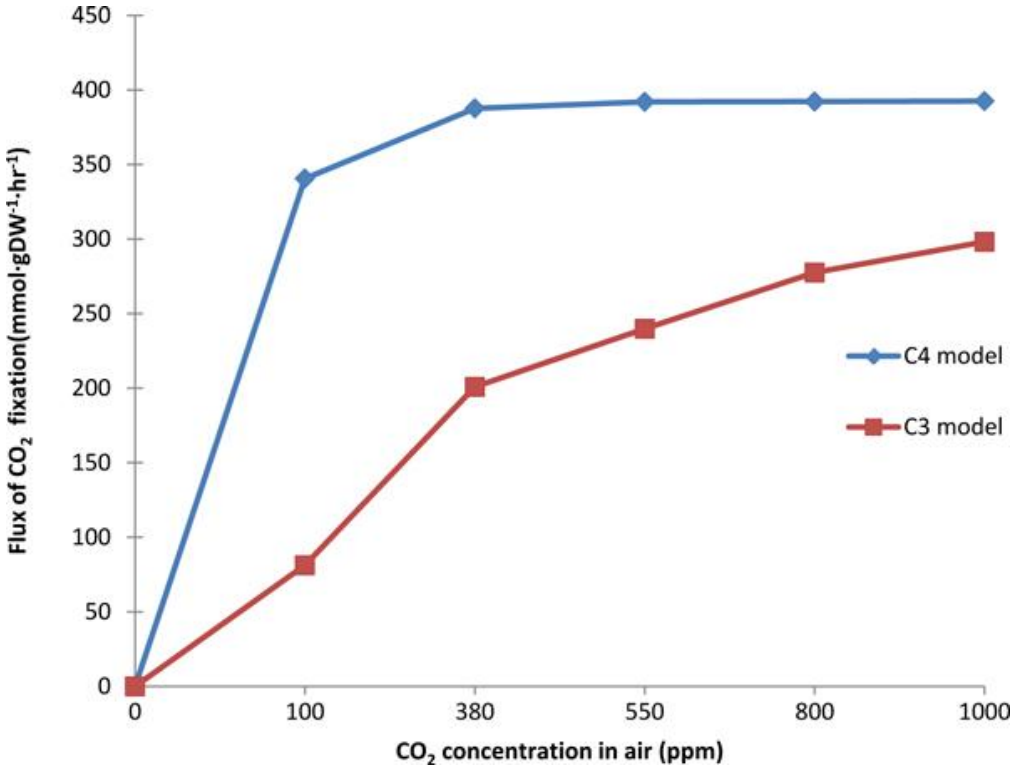

Figure10. *The effect of CO_2 concentration on CO_2 fixation in C3 and C4 model*

2.6. Contribution of Different C4 Subtypes to Biomass Production

C4 plants can be classified to three subtypes according to decarboxylation modes: NADP-malic enzyme (NADP-ME), NAD-malic enzyme (NAD-ME) and PEP carboxykinase (PCK). We explored the influence of each subtype on biomass synthesis and CO2 fixation, by blocking the flux of other two enzymes and giving enough supply of water and nitrogen. As shown in Table Table6,6, for each specific subtype, only the corresponding enzyme has flux and the other two enzymes have zero flux. There are little differences on biomass in the three subtypes. In comparison, the flux of biomass and

CO_2 fixation are maximal in PCK subtype. Moreover, when all the three subtypes are assumed to be active in one metabolism system, the PCK subtype is superior to be used for CO2 decarboxylation. These results are consistent with Fravolini's experiments that photosynthetic performance and above-ground biomass production of B.curtipendula, (PCK subtype) are greater than NADP-ME and NAD-ME types [43]. However, the photosynthesis and biomass of different subtypes also depend on environment conditions, including water and nitrogen supply [44,45]. For example, some species of NADP-ME type show higher rates of photosynthetic and biomass production under low nitrogen availability [46]. Therefore, to clearly elucidate the superiority of C4 subtypes, further design and analysis under multi-factorial combination of environment conditions are required.

Table6. *The influences of different C4 subtypes on flux of biomass synthesis and CO_2 fixation*

C4 subtypes	**NADP-ME**	**NAD-ME**	**PCK**	**Three Subtypes**
Flux of reactions (mmol·gDW^{-1}·hr^{-1})				
Biomass synthesis	4.52	4.49	4.75	4.90
CO2 fixation	92.20	91.59	96.94	100.01
R00216 (NADP-ME)	79.63	0.00	0.00	0.00
R00214(NAD-ME)	0.00	79.07	0.00	0.00
R00341 (PCK)	0.00	0.00	83.98	86.79

3. CONCLUSION

There is possibility to engineer C4 photosynthesis into C3 plants, because all C4 key enzymes are also present in C3 plants, although the expression levels are much lower than that in C4 species [1]. However it is an enormous challenge. To realize the transition from C3 to C4, systems biology will play a critical role in many aspects, including identification of key regulatory elements controlling development of C4 features and viable routine towards C4 using constraint-based modeling approach [47]. In this study, we improved the current metabolism models AraGEM and C4GEM by setting the ratio of carboxylation and oxygenation by Rubisco, and then systematically compared the constraint-based metabolic networks of C3 and C4 plants for the first time. We found C4 plants have less dense topology, higher robustness, better modularity, and higher CO_2 and radiation use efficiency, which provide important basis for engineering C4 photosynthesis into C3 plants. In addition, preliminary analysis indicated that the rate of CO2 fixation and biomass production in PCK subtype are superior to NADP-ME and NAD-ME subtypes under enough supply of water and nitrogen. All results are consistent with the actual situation, which indicate that Flux Balance Analysis is a useful method to analyze and compare large-scale metabolism systems of plants.

4. METHODS

4.1. Determination of the Ratio between Carboxylation and Oxygenation

We improved AraGEM and C4GEM by setting the ratio of carboxylation and oxygenation by Rubsico, which has not been conducted in any plant metabolic system. For C3 plants, the ratio r between carboxylation and oxygenation under specific CO_2 and O_2 concentration can be calculated by the following (4-6).

$$Vco2=co2co2+Kc(1+O2Ko) \quad (4)$$

$$Vo2=O2O2+Ko(1+co2Kc)*0.21 \quad (5)$$

$$r=Vco2Vo2 \quad (6)$$

Equation (5) and (6) include mechaelis constants for CO_2 with K_c = 460μbar and O_2 with K_o= 330mbar [28]. The O_2 concentration is 210 mbar and the intercellular CO_2 concentration is about 70 percent of CO_2 in air, which is 380μbar under standard condition. Unlike C3 plants, C4 photosynthesis requires the coordinated functioning of mesophyll and bundle sheath cells by CO_2 concentrating mechanism. The ratio r of carboxylation to oxygenation can be expressed as equation (7-15) [48]

$$Vp=\min\{Cm*Vpmax Cm+Kp,Vpr\} \quad (7)$$

$$Ac = \min\{(Vp + gs * Cm - Rm), (Vcmax - Rd)\} \quad (8)$$

$$Aj=(1-x)Jt3-Rd \quad (9)$$

$$A = \min\{A_c, A_j\} \quad (10)$$

if $Ac = Vp + gs * Cm - Rm$ (11)

$Cs=\gamma^{*}Os+Kc(1+Os/Ko)((Ac+Rd)/Vc\max)1-(Ac+Rd)/Vc\max$ (12)

$r=VcVo=Cs2\gamma^{*}Os$ (13)

else $Ac<Vp + gs^{*}Cm - Rm$ (14)

$r=VcVo=Cs2\gamma^{*}Os=Cm^{*}gs+Vp-A-Rm2\gamma^{*}(\alpha A0.047+Om^{*}gs)$ (15)

Where C_s and C_m are CO_2 partial pressures respectively in bundle sheath and mesophyll cells; $O_s$and O_m are O_2 partial pressures in the two cells; $V_p$is the rate of PEP carboxylation; V_{pmax}(120μmol·m^{-2}·s^{-1}) is the maximum PEP carboxylation rate; K_p(80μbar) is Michaelis constant of PEP carboxylase for CO_2; V_{pr}(80μmol·m^{-2}·s^{-1})is the constant rate of PEP regeneration; g_s(3mmol·m^{-2}·s^{-1}) is the physical conductance to CO_2 leakage; A_c is Rubisco-limited rate of CO_2 assimilation; $A_j$is electron-transport-limited rate; A is the CO_2 assimilation rate; V_{cmax}(60μmol·m^{-2}·s^{-1}) is the maximum Rubisco activity; γ (0.5/2590) is half the reciprocal of Rubisco specificity; R_d = 0.01V_{cmax} = 0.6μmol·m^{-2}·s^{-1} is leaf mitochondrial respiration; R_m = 0.5 R_d = 0.3μmol·m^{-2}·s^{-1} is mesophyll mitochondrial respiration; α ($0<\alpha<1$, α were assumed to be zero in our results) is fraction of PSII activity in the bundle sheath; x (x = 0.4) is partitioning factor of electron transport rate. J_{max}(400μmol electron m^{-2}·s^{-1}) is maximal electron transport rate; K_c (650μbar) for CO_2 and K_o(450mbar) for O_2 are mechaelis constants of Rubisco. In C4 plants, CO_2 concentration in mesophyll cell is only 37 percent of CO_2 in air [49] and the other parameters can be obtained in [48].

4.2. Topological Parameters in Metabolic Network

The topological properties of metabolic network can be analyzed based on graph theory, which can reflect the structure and robustness of large-scale network. In this study, the reactions are represented as nodes, if the product of reaction A is the substrate of a reaction B, there will be an edge from A to B. We consider some important parameters including degree, clustering coefficient, betweenness centrality and distance (path length). The degree of a node is the number of edges connected with other reactions. Degree centralization of a network is the variation in the degrees of vertices divided by the maximum degree variation which is possible in a network of the same size. Clustering coefficient is used to compute different inherent tendency coefficients in undirected network. Betweenness centralization is the variation in the betweenness centrality of vertices divided by the maximum variation in betweenness centrality possible in a network of the same size. The distance between two nodes is the shortest path length from one to the other. The diameter of network is the maximal distance among all pairs of nodes. All the topology analysis was conducted using the visual software Pajek [26].

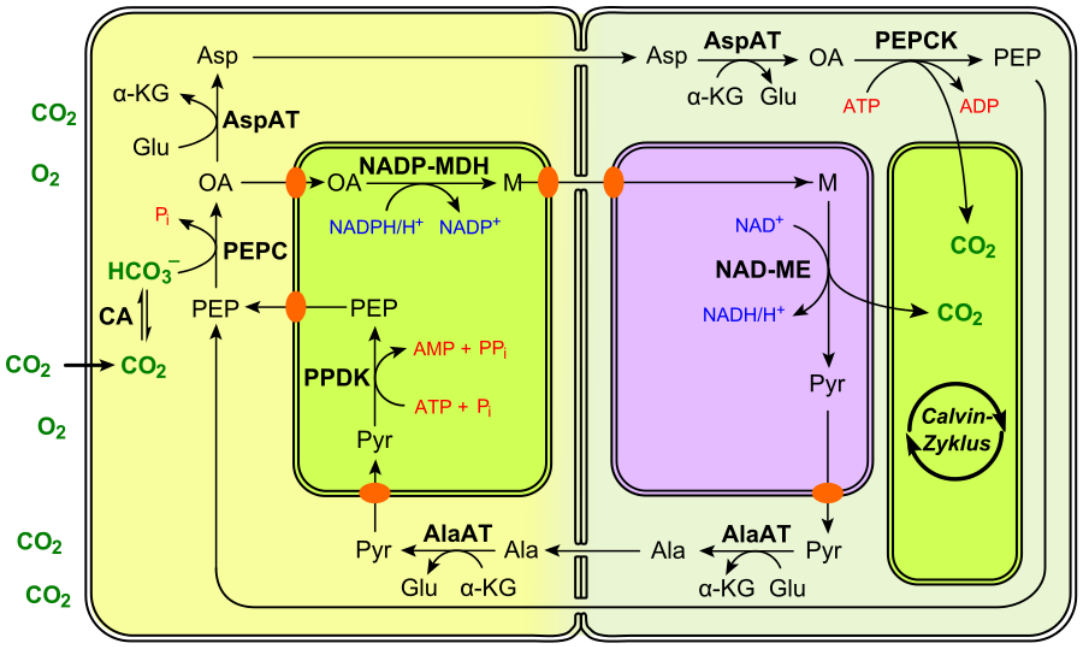

Figure11. *PEPCK type C_4 pathway*

4.3. Flux Balance Analysis

The biochemical reactions can be represented mathematically in the form of a stoichiometric matrix *S*, the flux through all reactions in a network is represented by the vector *v*, so the system of mass balance equation at steady state is given as $Sv = 0$. In any realistic large-scale metabolic model, there are more reactions than compounds, so there is no unique solution to this system of equations. Flux Balance Analysis (FBA) can solve the flux distribution by setting a set of upper and lower bounds on *v* and optimizing some objective function with linear programming, as following:

$$\text{Maximize or minimize } Z=c\ T v \text{subjectto } Sv=0 \text{andvm i } n\leq v\leq vm$$

Where *c* is a vector of weights indicating how much each reaction contributes to the objective function. In this study, we choose CO_2 fixation and biomass synthesis as two objective functions.

The COBRA toolbox is a free MATLAB toolbox for performing the simulation. The fluxes that are identified at various perturbations can be compared with each other and with experimental data.

4.4. Uniform Random Sampling

Uniform random sampling of the solution space in any environmental condition is a rapid and scalable way to characterize the structure of the allowed space of metabolic fluxes. Before the sampling was performed, the effective constraints for each reaction were calculated using the method of Flux Balance Analysis in COBRA toolbox [50]. Specifically in sampling, COBRA toolbox uses an implementation of the artificial centered hit-and-run (ACHR) sampler algorithm with slight modifications to generate such a set of flux distributions that uniformly sample the space of all feasible fluxes. Initially, a set of 5000 non-uniform pseudo-random points, called warm-up points, was generated. In a series of iterations, each point was randomly moved while keeping it within the feasible flux space. This was accomplished by choosing a random direction, computing the limits on how far a point could travel in that direction (positive or negative), and then choosing a new point randomly along that line. After numerous iterations, the set of points was mixed and approached a uniform sample of the solution space [51] and 2000 points was loaded for analysis. The sampling procedure can be achieved with the function 'sample CbModel' and the correlated reaction sets can be identified by 'identifyCorrelSets' in the COBRA toolbox. Correlated reaction sets are mathematically defined as modules in biochemical reaction network which facilitate the study of biological processes by decomposing complex reaction networks into conceptually simple units. This sampling approach is used to fully determine the range of possible distributions of steady-state fluxes allowed in the network under defined physicochemical constraints and used to analyze the general properties of networks by testing

ACKNOWLEDGEMENTS

We thank Semnan University for providing us the SBML file of C4GEM model which can be loaded into COBRA toolbox.

REFERENCES

[1] Kajala K, Covshoff S, Karki S, Woodfield H, Tolley BJ, Dionora MJ, Mogul RT, Mabilangan AE, Danila FR, Hibberd JM, Quick WP. Strategies for engineering a two-celled C4 photosynthetic pathway into rice. J Exp Bot. 2011; 62:3001–3010. doi: 10.1093/jxb/err022. [PubMed] [Cross Ref]

[2] Majeran W, Friso G, Ponnala L, Connolly B, Huang M, Reidel E, Zhang C, Asakura Y, Bhuiyan NH, Sun Q, Turgeon R, van Wijk KJ. Structural and metabolic transitions of C4 leaf development and differentiation defined by microscopy and quantitative proteomics in maize. Plant Cell. 2010; 22:3509–3542. doi: 10.1105/tpc.110.079764. [PMC free article] [PubMed] [Cross Ref]

[3] Hibberd JM, Sheehy JE, Langdale JA. Using C4 photosynthesis to increase the yield of rice-rationale and feasibility. CurrOpin Plant Biol. 2008; 11:228–231. doi: 10.1016/j.pbi.2007.11.002. [PubMed] [Cross Ref]

[4] Taniguchi Y, Ohkawa H, Masumoto C, Fukuda T, Tamai T, Lee K, Sudoh S, Tsuchida H, Sasaki H, Fukayama H, Miyao M. Overproduction of C4 photosynthetic enzymes in transgenic rice plants: an approach to introduce the C4-like photosynthetic pathway into rice. J Exp Bot. 2008; 59:1799–1809. [PubMed]

[5] Evans JR. Enhancing C3 photosynthesis. Plant Physiol. 2010; 154:589–592. doi: 10.1104/pp.110.160952. [PMC free article] [PubMed] [Cross Ref]

[6] Sweetlove LJ, Last RL, Fernie AR. Predictive metabolic engineering: a goal for systems biology. Plant Physiol. 2003; 132:420–425. doi: 10.1104/pp.103.022004. [PMC free article] [PubMed] [Cross Ref]

[7] Gutierrez RA, Shasha DE, Coruzzi GM. System's biology for the virtual plant. Plant Physiol. 2005; 138:550–554. doi: 10.1104/pp.104.900150. [PMC free article] [PubMed] [Cross Ref]

[8] DellaPenna D. Plant metabolic engineering. Plant Physiol. 2001; 125:160–163. doi: 10.1104/pp.125.1.160. [PMC free article] [PubMed] [Cross Ref]

[9] Kitano H. Standards for modeling. Nat Biotechnol. 2002; 20:337. [PubMed]

[10] Kitano H. System's biology: a brief overview. Science. 2002; 295:1662–1664. doi: 10.1126/science.1069 492. [PubMed] [Cross Ref]

[11] Dennis C, Surridge C. Arabidopsis thaliana genome. Introduction. Nature. 2000; 408:791. [PubMed]

[12] Paterson AH, Bowers JE, Bruggmann R, Dubchak I, Grimwood J, Gundlach H, Haberer G, Hellsten U, Mitros T, Poliakov A, Schmutz J, Spannagl M, Tang H, Wang X, Wicker T, Bharti AK, Chapman J, Feltus FA, Gowik U, Grigoriev IV, Lyons E, Maher CA, Martis M, Narechania A, Otillar RP, Penning BW, Salamov AA, Wang Y, Zhang L, Carpita NC. et al. The Sorghum bicolor genome and the diversification of grasses. Nature. 2009; 457:551–556. doi: 10.1038/nature07723. [PubMed] [Cross Ref]

[13] Becker SA, Feist AM, Mo ML, Hannum G, Palsson BØ, Herrgard MJ. Quantitative prediction of cellular metabolism with constraint-based models: the COBRA Toolbox. Nature Protocols. 2007; 2:727–738. doi: 10.1038/nprot.2007.99. [PubMed] [Cross Ref]

[14] Boyle NR, Morgan JA. Flux balance analysis of primary metabolism in Chlamydomonasreinhardtii. BMC SystBiol. 2009; 3:4. [PMC free article] [PubMed]

[15] Pramanik J, Keasling JD. Stoichiometric model of Escherichia coli metabolism: incorporation of growth-rate dependent biomass composition and mechanistic energy requirements. BiotechnolBioeng. 1997; 56:398–421. [PubMed]

[16] Varma A, Palsson BO. Stoichiometric flux balance models quantitatively predict growth and metabolic by-product secretion in wild-type Escherichia coli W3110. Appl Environ Microbiol. 1994; 60:3724–3731. [PMC free article] [PubMed]

[17] Price ND, Papin JA, Schilling CH, Palsson BO. Genome-scale microbial in silico models: the constraints-based approach. Trends Biotechnol. 2003; 21:162–169. doi: 10.1016/S0167-7799(03)00030-1. [PubMed] [Cross Ref]

[18] Grafahrend-Belau E, Schreiber F, Koschutzki D, Junker BH. Flux balance analysis of barley seeds: a computational approach to study systemic properties of central metabolism. Plant Physiol. 2009; 149:585–598. doi: 10.1104/pp.108.129635. [PMC free article] [PubMed] [Cross Ref]

[19] De Oliveira Dal'Molin CG, Quek LE, Palfreyman RW, Brumbley SM, Nielsen LK. AraGEM, a Genome-Scale Reconstruction of the Primary Metabolic Network in Arabidopsis. Plant Physiology. 2009; 152:579–589. [PMC free article] [PubMed]

[20] Poolman MG, Miguet L, Sweetlove LJ, Fell DA. A genome-scale metabolic model of Arabidopsis and some of its properties. Plant Physiol. 2009; 151:1570–1581. doi: 10.1104/pp.109.141267. [PMC free article] [PubMed] [Cross Ref]

[21] Radrich K, Tsuruoka Y, Dobson P, Gevorgyan A, Swainston N, Baart G, Schwartz JM. Integration of metabolic databases for the reconstruction of genome-scale metabolic networks. BMC SystBiol. 2010; 4:114. [PMC free article] [PubMed]

[22] Williams TC, Poolman MG, Howden AJ, Schwarzlander M, Fell DA, Ratcliffe RG, Sweetlove LJ. A genome-scale metabolic model accurately predicts fluxes in central carbon metabolism under stress conditions. Plant Physiol. 2010; 154:311–323. doi: 10.1104/pp.110.158535. [PMC free article] [PubMed] [Cross Ref]

[23] Knoop H, Zilliges Y, Lockau W, Steuer R. The metabolic network of Synechocystis sp. PCC 6803: systemic properties of autotrophic growth. Plant Physiol. 2010; 154:410–422. doi: 10.1104/pp.110.157198. [PMC free article] [PubMed] [Cross Ref]

[24] Golomysova A, Gomelsky M, Ivanov PS. Flux balance analysis of photoheterotrophic growth of purple nonsulfur bacteria relevant to biohydrogen production. International Journal of Hydrogen Energy. 2010; 35:12751–12760. doi: 10.1016/j.ijhydene.2010.08.133. [Cross Ref]

[25] de Oliveira Dal'Molin CG, Quek LE, Palfreyman RW, Brumbley SM, Nielsen LK. C4GEM, a Genome-Scale Metabolic Model to Study C4 Plant Metabolism. Plant Physiology. 2010; 154:1871–1885. doi: 10.1104/pp.110.166488. [PMC free article] [PubMed] [Cross Ref]

[26] Mrvar A, Batagelj V. Exploratory network analysis with pajek. Mark Granovetter: Cambridge University Press; 2005.

[27] Albert R, DasGupta B, Hegde R, Sivanathan GS, Gitter A, Gürsoy G, Paul P, Sontag E. A new computationally efficient measure of topological redundancy of biological and social networks. Physical Review E. 2011; 84:036117. [PubMed]

[28] Farquhar GD, Berry JA. A Biochemical Model of Photosynthetic CO2 Assimilation in Leaves of C3 Species. Planta. 1980; 149:78–90. doi: 10.1007/BF00386231. [PubMed] [Cross Ref]

[29] Marri L, Sparla F, Pupillo P, Trost P. Co-ordinated gene expression of photosynthetic glyceraldehyde-3-phosphate dehydrogenase, phosphoribulokinase, and CP12 in Arabidopsis thaliana. J Exp Bot. 2005; 56:73–80. [PubMed]

[30] GeneBank Database. http://www.ncbi.nlm.nih.gov/gene/

[31] Quick WP, Schurr U, Fichtner K, Schulze E-D, Rodermel SR, Bogorad L, Stitt M. The impact of decreased Rubisco on photosynthesis, growth, allocation and storage in tobacco plants which have been transformed with antisense *rbcS*. The Plant Journal. 1991; 1:51–58. doi: 10.1111/j.1365-313X.1991.00051.x. [Cross Ref]

[32] Sicher RC, Bunce JA. Relationship of photosynthetic acclimation to changes of Rubisco activity in field-grown winter wheat and barley during growth in elevated carbon dioxide. PHOTOSYNTHESIS RESEARCH. 1997; 52:27–38. doi: 10.1023/A:1005874932233. [Cross Ref]

[33] Debnam PM, Emes MJ. Subcellular distribution of enzymes of the oxidative pentose phosphate pathway in root and leaf tissues. Journal of Experimental Botany. 1999; 50:1653–1661.

[34] Zelitch I, Schultes NP, Peterson RB, Brown P, Brutnell TP. High glycolate oxidase activity is required for survival of maize in normal air. Plant Physiol. 2009; 149:195–204. doi: 10.1104/pp.108.128439. [PMC free article] [PubMed] [Cross Ref]

[35] CLORE SMD AM, TINNIRELLO SMN. Increased levels of reactive oxygen species and expression of a cytoplasmic aconitase/iron regulatory protein 1 homolog during the early response of maize pulvini to gravistimulation. Plant, Cell & Environment. 2008; 31:144–158. [PubMed]

[36] Schwarte S, Bauwe H. Identification of the photorespiratory 2-phosphoglycolate phosphatase, PGLP1, in Arabidopsis. Plant Physiol. 2007; 144:1580–1586. doi: 10.1104/pp.107.099192. [PMC free article] [PubMed] [Cross Ref]

[37] Lunn JE, Ashton AR, Hatch MD, Heldt HW. Purification, molecular cloning, and sequence analysis of sucrose-6F-phosphate phosphohydrolase from plants. PNAS. 2000; 97:12914–12919. doi: 10.1073/pnas.230430197. [PMC free article] [PubMed] [Cross Ref]

[38] Hernández JMGM, Castignolles P, Gidley MJ, Myers AM, Gilbert RG. Mechanistic investigation of a starch-branching enzyme using hydrodynamic volume SEC analysis. Biomacromolecules. 2008; 9:954–965. doi: 10.1021/bm701213p. [PubMed] [Cross Ref]

[39] Monreal JA, McLoughlin F, Echevarria C, Garcia-Maurino S, Testerink C. Phosphoenolpyruvate carboxylase from C4 leaves is selectively targeted for inhibition by anionic phospholipids. Plant Physiol. 2010; 152:634–638. doi: 10.1104/pp.109.150326. [PMC free article] [PubMed] [Cross Ref]

[40] Mechin V, Thevenot C, Le Guilloux M, Prioul JL, Damerval C. Developmental analysis of maize endosperm proteome suggests a pivotal role for pyruvate orthophosphate dikinase. Plant Physiol. 2007; 143:1203–1219. doi: 10.1104/pp.106.092148. [PMC free article] [PubMed] [Cross Ref]

[41] Oberhuber W, Dai Z-Y, Edwards GE. Light dependence of quantum yields of Photosystem II and CO2 fixation in C3 and C4 plant. Photosythesis research. 1993; 35:265–274. doi: 10.1007/BF00016557. [PubMed] [Cross Ref]

[42] Kanai R, Edwards GE. The biochemistry of C4 photosynthesis. Chapter 3 in C4 Plant Biology. . 1999.

[43] Fravolini A, Williams DG, Thompson TL. Carbon isotope discrimination and bundle sheath leakiness in three C4 subtypes grown under variable nitrogen, water and atmospheric CO2 supply. Journal of Experimental Botany. 2002; 53:2261–2269. doi: 10.1093/jxb/erf084. [PubMed] [Cross Ref]

[44] Bowman WD. Inputs and Storage of Nitrogen in Winter Snowpack in an Alpine Ecosystem. Arctic and Alpine Research. 1992; 24:211–215. doi: 10.2307/1551659. [Cross Ref]

[45] Buchman N, Brooks JR, Rapp KD, Ehleringer JR. Carbon isotope composition of C4 grasses is influenced by light and water supply. Plant, Cell & Environment. 1996; 19:392–402. doi: 10.1111/j.1365-3040.1996.tb00331.x. [Cross Ref]

[46] Taub DR, Lerdau MT. Relationship between leaf nitrogen and photosynthetic rate for three NAD-ME and three NADP-ME C4 grasses. Am J Bot. 2000; 87:412–417. doi: 10.2307/2656637. [PubMed] [Cross Ref]

[47] Zhu XG, Shan L, Wang Y, Quick WP. C4 rice - an ideal arena for systems biology research. J Integr Plant Biol. 2010; 52:762–770. doi: 10.1111/j.1744-7909.2010.00983.x. [PubMed] [Cross Ref]

[48] Caemmerer SV. Modeling C4 photosynthesis. In Biochemical models of leaf photosynthesis. 2000. pp. 91–122.

[49] Ziska LH, Bunce JA. Influence of increasing carbon dioxide concentration on the photosynthetic and growth stimulation of selected C4 crops and weeds. Photosynthesis Research. 1997; 54:199–208. doi: 10.1023/A:1005947802161. [Cross Ref]

[50] Price ND, Schellenberger J, Palsson BO. Uniform sampling of steady-state flux spaces: means to design experiments and to interpret enzymopathies. Biophys J. 2004; 87:2172–2186. doi: 10.1529/biophysj.104.043000. [PMC free article] [PubMed] [Cross Ref]

[51] Schellenberger J, Lewis NE, Palsson BO. Elimination of thermodynamically infeasible loops in steady-state metabolic models. Biophys J. 2011; 100:544–553. doi: 10.1016/j.bpj.2010.12.3707. [PMC free article] [PubMed] [Cross Ref]

Citation: *Hamid kheyrodin. (2018). Comparison of C3 and C4 Plants Metabolic. International Journal of Research Studies in Agricultural Sciences (IJRSAS), 4(6), pp.8-22, http://dx.doi.org/10.20431/2454-6224.0406002*